Gait Generation via Intrinsically Stable MPC for a Multi-Mass Humanoid Model

Nicola Scianca, Valerio Modugno, Leonardo Lanari, Giuseppe Oriolo

***Abstract*— We consider the problem of generating a gait with no a priori assigned footsteps while taking into account the contribution of the swinging leg to the total Zero Moment Point (ZMP). This is achieved by considering a multi-mass model of the humanoid and distinguishing between secondary masses with known pre-defined motion and the remaining, primary, masses. In the case of a single primary mass with constant height, it is possible to transform the original gait generation problem for the multi-mass system into a single LIP-like problem. We can then take full advantage of an intrinsically stable MPC framework to generate a gait that takes into account the swinging leg motion.**

I. Introduction

The number of possible applications and the interest for humanoid robots has grown constantly in the last decade. However, while other robotic platforms have reached impressive results, most humanoids still seem to move quite poorly due to their peculiar characteristics: difficulty in maintaining balance and walking robustly. Therefore gait generation for humanoids is still a very active research area.

One of the most widely used criteria for generating gaits is based on the Zero Moment Point (ZMP) and the non-tilting condition [1] which requires the ZMP to remain within the robot support polygon. It is however possible to highlight two distinctive aspects in the gait generation problem: the generation of a ZMP trajectory compatible with the non-tilting constraint and the determination of a corresponding stable Center of Mass (CoM) trajectory. Once a desired CoM trajectory is generated, one may use kinematic control to generate joint commands that will drive the robot along it.

A possible distinction in the gait generation problem can be made depending if the future steps have already been decided or not. In particular, if the future footsteps have been planned in advance then an interpolating desired ZMP trajectory can be readily obtained such that at any instant the ZMP remains within the support polygon in both the single and the double support phase. This situation is usually known as *assigned footsteps problem*. If no footstep adaptation is possible, this solution is not very robust and no reactivity is possible.

A more challenging problem consists in deciding simultaneously the footsteps placement (and therefore the ZMP) and the corresponding CoM stable behavior. This corresponds to a simultaneous CoM/ZMP planning problem [2] or *automatic footsteps problem* [3]. Such a solution allows continuous adaptation of the current gait to disturbances and modeling errors.

The authors are with the Dipartimento di Ingegneria Informatica, Automatica e Gestionale, Sapienza Università di Roma, via Ariosto 25, 00185 Roma, Italy. E-mail: *lastname*@diag.uniroma1.it. This work is supported by the EU FP7 project COMANOID.

In all cases, the accuracy of the ZMP computation, due to its fundamental role in the non-tilting condition, plays an important role. Real-time gait generation however requires a compromise between model complexity and speed. The simplest and most widely used model considers the whole system CoM motion while assuming its height constant and neglecting its inertia. This leads to the Linear Inverted Pendulum (LIP) [4]. A more accurate expression of the ZMP can be achieved by increasing the number of considered point masses with negligible inertia: the multi-mass model. Due to its important effect on the overall ZMP, 2- or 3-mass models have been typically used to model the effect of the swinging leg motion.

One of the first off-line multi-mass based gait generation approach compensates for all other limbs influence by using either the trunk motion alone [5] or by also considering the waist motion to overcome actuator limitations in the trunk [6]. An on-line trajectory generation algorithm has been introduced in [7], neglecting the acceleration of the swinging leg and thus obtaining a gravity compensation which reduces the problem to that of a particular LIP. The same idea of maintaining a linear model to derive the CoM has been used in [8] but considering also multiple masses. Other significant contributions have followed as [9], [10] who find the body center of mass reference trajectory for assigned footsteps or [11] who introduces first the divergent component of motion and compensates for the swing foot contribution. Multiple constant height masses have been considered in [12] while the preview control approach of Kajita [4] has been extended to the 3-mass problem in [13] where the gain in accuracy was comparable to the multiple preview stages results.

Most of these papers differ not only in the approximations used but also in how the CoM trajectory is obtained. We have, for both the assigned and free footsteps cases, briefly illustrated in [14], [15] how a recent result [16], which shows how the ZMP and every corresponding bounded CoM evolution are related through a so-called *boundedness constraint*, can be used for compensating the swing foot motion.

The alternative setting of Model Predictive Control has also been used with multi-mass modeling in [17] and most recently in [18]. Clear advantages of MPC-based algorithms w.r.t. preview control include shorter prediction horizons thus allowing online reactive behaviors and most notably the possibility to deal with constraints.

In this paper we embed a multi-mass model in our

intrinsically stable MPC. This framework, proposed in [19] and further developed in [20], is capable of generating a gait while guaranteeing that the resulting CoM motion is bounded, even for a very short prediction horizon. We are therefore able to generate a gait with automatic footsteps while taking into account the motion of the swinging leg. Moving within an MPC framework allows the inclusion of explicit constraints and cost functions.

The paper is organized as follows: we start in Sec. II with a general multi-mass modeling approach which will lead to the *equivalent LIP* system and a simplified gait generation problem formulation. This problem will be solved in Sec. III and applied to the gait generation of a humanoid while taking into account the motion of the swinging leg for the automatic footsteps case. Simulations will follow in Sec. IV which provides a first set of useful comparative results. Conclusions and future work are finally reported.

II. Humanoid multi-mass modeling

In the following sections we will first briefly recall the multi-mass approach to modeling that will be used in this paper for taking into account the motion of the swinging leg during the single support phase. The resulting 2-mass system is then recast as an equivalent LIP, which is then used to derive the stability constraint that characterizes bounded motions.

A. Moment balance and ZMP computation

A common approach to simplify the computation of the ZMP consists in neglecting the inertia of each link around its center of mass, therefore considering the robot as a collection of N point masses m_i. Typically a number of masses, defined as *secondary* and usually associated to limbs, have predefined relative motions in an inertial frame (e.g., w.r.t. the stance foot). The system motion must be specified in terms of the remaining masses, defined as *primary*.

Typical cases are:

- $N = 1$. Only the motion of a single mass concentrated at the humanoid CoM is considered; the resulting system is the Inverted Pendulum (IP). Under the additional constraint of constant CoM height, the model becomes linear and is known as the Linear Inverted Pendulum (LIP). Clearly, there are no secondary masses.
- $N = 2$. The primary mass represents the main body and the secondary the swinging leg (see, e.g., [5], [9]). Alternatively, the primary mass can represent the humanoid and the secondary a heavy carried load with either known contact forces or motion [21].
- $N = 3$. The primary mass represents the main body as the primary mass and each of the two secondary masses represents a leg. The main difference with the $N = 2$ case lies in how the double support phase is modeled. Another instance of this case is a walking biped carrying a human as a 'walking wheelchair', with the primary mass standing for the humanoid plus the passenger body, while the two secondary masses represent the passenger legs [22].

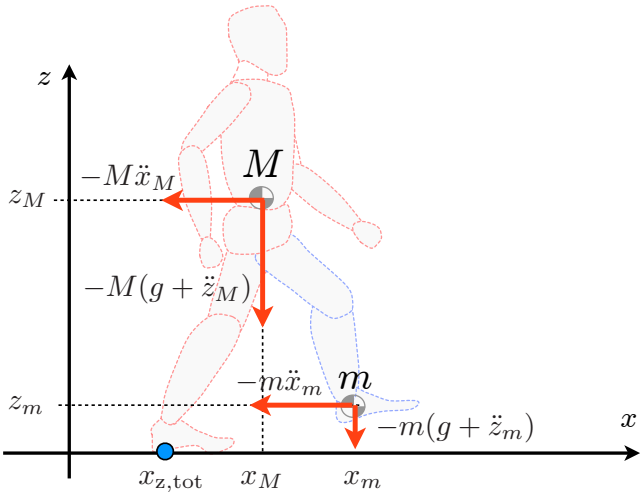

Fig. 1. 2-mass model in the sagittal plane.

- $N > 3$. More accurate models can be built by further distinguishing the different humanoid components (trunk, waist, feet, legs, arms, head) as in [6], clearly at the expense of an increased computational cost.

Consider the case $N = 2$ in the sagittal plane[1] (x, z), and refer to Fig. 1. Let (x_M, z_M) and (x_m, z_m) denote the coordinates respectively of M and m. The total ZMP coordinate $x_{z,tot}$ of the 2-mass system is obtained from the moment balance during single support

$$\begin{aligned} Mz_M\ddot{x}_M - M(g+\ddot{z}_M)(x_M - x_{z,tot}) + \\ mz_m\ddot{x}_m - m(g+\ddot{z}_m)(x_m - x_{z,tot}) = 0 \end{aligned} \quad (1)$$

where g is the gravitational constant. Note that when vertical acceleration of a mass (either $\ddot{z}_M$ or $\ddot{z}_m$) is equal to $-g$, its contribution to the ZMP will be zeroed. This corresponds to a *free fall* of the mass and thus unlikely to happen in a normal gait.

Define

$$x_{z,M} = x_M - \frac{z_M}{\ddot{z}_M + g}\ddot{x}_M \quad (2)$$

$$x_{z,m} = x_m - \frac{z_m}{\ddot{z}_m + g}\ddot{x}_m \quad (3)$$

One can interpret (2) as the motion equation of an IP of mass M, variable height z_M and ZMP $x_{z,M}$; a similar interpretation holds for in (3) with m in place of M.

Equation (1) can now be rearranged as

$$(\ddot{z}_M + g)(x_{z,tot} - x_{z,M}) = \frac{m}{M}(\ddot{z}_m + g)(x_{z,m} - x_{z,tot}) \quad (4)$$

Here, $x_{z,tot} - x_{z,M}$ represents the contribution of m to the total ZMP. We can solve (4) for $x_{z,tot}$ as

$$x_{z,tot} = \left(1 + \frac{m}{M}\frac{\ddot{z}_m + g}{\ddot{z}_M + g}\right)^{-1}\left(x_{z,M} + \frac{m}{M}\frac{\ddot{z}_m + g}{\ddot{z}_M + g}x_{z,m}\right) \quad (5)$$

[1]Motions in the sagittal and coronal plane are decoupled and therefore the same derivations can be carried out in the coronal plane (y, z).

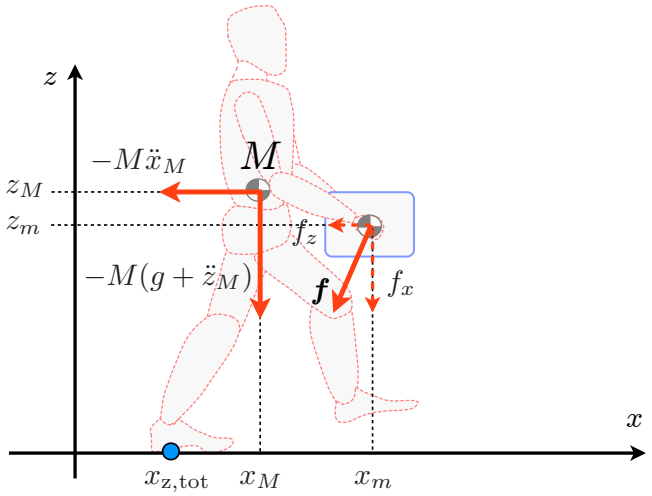

Fig. 2. 2-mass model with external force $\boldsymbol{f}^T = (f_x, f_z)$ applied in (x_m, z_m).

It is important to stress that this total ZMP differs from the ZMP of an IP with mass $m+M$ concentrated in $(x_\mathrm{c}, z_\mathrm{c})$

$$x_\mathrm{c} = \frac{Mx_M + mx_m}{m+M}, \qquad z_\mathrm{c} = \frac{Mz_M + mz_m}{m+M} \tag{6}$$

i.e., at the CoM of our 2-mass model. In fact, the corresponding ZMP $x_{z,\mathrm{IP}}$ satisfies the following moment balance

$$(m+M)z_\mathrm{c}\ddot{x}_\mathrm{c} - (m+M)(g+\ddot{z}_\mathrm{c})(x_\mathrm{c} - x_{z,\mathrm{IP}}) = 0 \tag{7}$$

which, using (6), can be shown to differ from (1). The difference $x_{z,\mathrm{tot}} - x_{z,\mathrm{IP}}$ can be regarded as an increase in ZMP prediction accuracy obtained by moving from the 1-mass IP to the 2-mass model.

A formally equivalent moment balance can be written when an external force $\boldsymbol{f}^T = (f_x, f_z)$ acts on the humanoid at a generic point (x_m, z_m), as shown in Fig. 2:

$$\begin{aligned} Mz_M\ddot{x}_M - M(g+\ddot{z}_M)(x_M - x_{z,\mathrm{tot}}) - \\ z_m f_x + (x_m - x_{z,\mathrm{tot}})f_z = 0 \end{aligned} \tag{8}$$

with the ZMP becoming

$$x_{z,\mathrm{tot}} = \left(1 - \frac{f_z}{M(\ddot{z}_M + g)}\right)^{-1}\left(x_{z,M} - \frac{x_m f_z - z_m f_x}{M(\ddot{z}_M + g)}\right) \tag{9}$$

as in [21], [23].

The previous modeling approach can be extended to the case of N masses with a single primary mass M (e.g. [4]). Denoting by (x_i, z_i) the coordinates of the i-th secondary mass m_i, the total ZMP can be rewritten in a form that generalizes (5):

$$x_{z,\mathrm{tot}} = \left(1 + \sum_{i=1}^{N-1} \frac{m_i}{M}\frac{\ddot{z}_i + g}{\ddot{z}_M + g}\right)^{-1}\left(x_{z,M} + \sum_{i=1}^{N-1} \frac{m_i}{M}\frac{\ddot{z}_i + g}{\ddot{z}_M + g}x_{z,i}\right)$$

where $x_{z,i}$ represents the equivalent of (3) for each mass m_i.

B. Equivalent LIP

Going back to the case $N = 2$, assume a constant height z_M for the primary mass to obtain a linear system and thus (4) leads to the well-known LIP equation which will be called *equivalent LIP*

$$x_M - \frac{1}{\omega_\mathrm{M}^2}\ddot{x}_M = x_{z,M} \tag{10}$$

where $\omega_M^2 = g/z_M$ and

$$x_{z,M} = x_{z,\mathrm{tot}} + \frac{m}{M}\left(\frac{\ddot{z}_m + g}{g}\right)(x_{z,\mathrm{tot}} - x_{z,m}) \tag{11}$$

In [14], [15] the total desired ZMP $x_{z,\mathrm{tot}}$ was assigned and $x_{z,M}$ becomes a known function of time which can be interpreted as an equivalent ZMP. The gait generation problem then reduces to finding a bounded solution to (10) forced by $x_{z,M}$.

In this paper, following the approach of [19], the ZMP derivative $\dot{x}_{z,M}$ of the primary mass is going to be chosen as a decision variable in the MPC formulation. It is therefore useful to recall how $x_{z,M}$ relates to $x_{z,\mathrm{tot}}$ through the moment balance (5) under the constant height z_M assumption

$$x_{z,\mathrm{tot}} = \left(1 + \frac{m}{M}\frac{\ddot{z}_m + g}{g}\right)^{-1}\left(x_{z,M} + \frac{m}{M}\frac{\ddot{z}_m + g}{g}x_{z,m}\right) \tag{12}$$

This relation will be used in Sec. III-B to define the constraint on the total ZMP in terms of the decision variable $x_{z,M}$.

C. Stability constraint

We recall how to derive a characterization of the bounded CoM trajectories associated to a given ZMP trajectory. The generic solution x_M of the LIP equation (10) will diverge in general. However it has been shown in [16] that there are some particular solutions satisfying the *stability constraint*

$$x_M(t_i) + \frac{\dot{x}_M(t_i)}{\omega_M} = \omega_M \int_{t_i}^{\infty} e^{-\omega_M(\tau - t_i)} x_{z,M}(\tau) d\tau \tag{13}$$

which will remain bounded for all $t \geq t_i$. Note that (13) requires future values of the ZMP $x_{z,M}$. This stability constraint, which characterizes *every* bounded CoM trajectory, has been included in the MPC formulation thus defining the *intrinsically stable* MPC. The reader should refer to [16], [19] for further details.

III. Intrinsically Stable MPC

In Sec. II-B an equivalent LIP model (10) which accounts for the swing leg motion has been defined. In the following we adapt the MPC algorithm presented in [19] and consider the case when the footsteps are not decided a priori but are the result of the optimization problem. Therefore we choose as control variables the ZMP time derivative of the primary mass, $(\dot{x}_{z,M}, \dot{y}_{z,M})$ together with the positions of the predicted footsteps x_f^j, y_f^j, with j denoting the j-th footstep. Both the sagittal and coronal plane are considered. Note that the total ZMP $(x_{z,\mathrm{tot}}, y_{z,\mathrm{tot}})$ is not pre-defined so it can adapt to changes or modeling errors when needed and simultaneously guarantee the non-tilting condition as in a simultaneous CoM/ZMP planning problem.

A. Motion model

The motion model for the MPC consists of the equivalent LIP (10) plus a dynamic extension to obtain smoother trajectories, i.e. we consider the following third order system

$$\begin{pmatrix} \dot{x}_M \\ \ddot{x}_M \\ \dot{x}_{\mathrm{z},M} \end{pmatrix} = \begin{pmatrix} 0 & 1 & 0 \\ \omega_M^2 & 0 & -\omega_M^2 \\ 0 & 0 & 0 \end{pmatrix} \begin{pmatrix} x_M \\ \dot{x}_M \\ x_{\mathrm{z},M} \end{pmatrix} + \begin{pmatrix} 0 \\ 0 \\ 1 \end{pmatrix} \dot{x}_{\mathrm{z},M}. \tag{14}$$

Following [19], we use piecewise-constant control over time intervals of duration δ, $\dot{x}_{\mathrm{z},M}(t) = \dot{x}^i_{\mathrm{z},M}$, for $t \in [t_i, t_{i+1})$, with $t_i = i\delta$, $i = 0, 1, \ldots$ and thus $x_{\mathrm{z},M}$ is given by

$$x_{\mathrm{z},M}(t) = x^i_{\mathrm{z},M} + (t - t_i)\, \dot{x}^i_{\mathrm{z},M}, \quad t \in [t_i, t_{i+1}). \tag{15}$$

The generic MPC iteration will plan for the time interval from the current sampling instant t_k to $t_{k+N} = t_k + T_\mathrm{h}$, where $T_\mathrm{h} = N \cdot \delta$ is the *prediction horizon*. We denote by $x^k_{\mathrm{z},M}$ the value of $x_{\mathrm{z},M}$ at the current instant $t = k\delta$ while $x^{k+i}_{\mathrm{z},M}$ will represent the predicted value i samples in the future.

B. Constraints

The constraints that are ensured during the optimization problem can be distinguished into:

- *ZMP constraint*. The primary mass ZMP and the footsteps have to be chosen in order to guarantee that the total ZMP $x_{\mathrm{z,tot}}$ always stays inside the support polygon.
- *Stability constraint*. The ZMP constraint alone does not guarantee boundedness of the resulting primary mass CoM motion. This is achieved by properly including the stability constraint (13) into the optimization problem.
- *Feasibility constraint*. The footsteps chosen by the algorithm need to be admissible.

For clarity of exposition, we focus only on one side of the ZMP constraint. At the generic instant i within the prediction horizon, we need to guarantee that

$$x^{k+i}_{\mathrm{z,tot}} - x^j_\mathrm{f} \leq \frac{1}{2} x^{\max}_\mathrm{z} \tag{16}$$

with x^j_f the position of the j-th footstep in the current prediction horizon and $x^{\max}_\mathrm{z}$ the size of the constraint. To use relation (12) between $x_{\mathrm{z,tot}}$ and the control variable $x_{\mathrm{z},M}$, we need to define the swing foot trajectory explicitly. When the foot moves from position x^{j-2}_f to x^j_f, we can write

$$x_m(t) = x^{j-2}_\mathrm{f} + p(t)(x^j_\mathrm{f} - x^{j-2}_\mathrm{f}), \quad \text{for} \quad t \in [0, t_\mathrm{ss}] \tag{17}$$

where t_ss is the single support duration. Here $p(t) \in [0, 1]$ is a monotonically increasing timing law of the swinging motion along x. The swing foot z-coordinate is given by

$$z_m(t) = -\frac{4 z^{\max}_m}{t^2_\mathrm{ss}} t(t - t_\mathrm{ss}), \quad \text{for} \quad t \in [0, t_\mathrm{ss}] \tag{18}$$

where $z^{\max}_m$ is the maximum height reached by the secondary mass. The timing law $p(t)$ and $z_m(t)$ are reported in Fig. 3. The foot trajectory plays an important role in the gait generation and requires a deeper analysis [24], [25] .

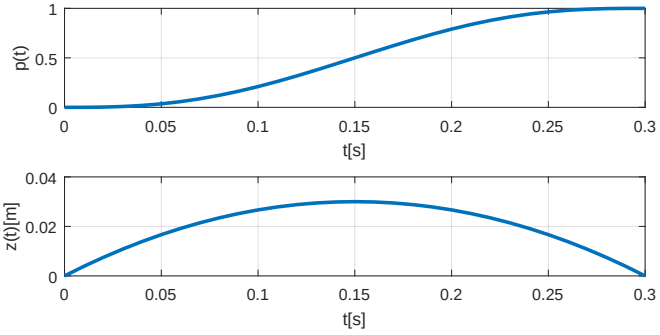

Fig. 3. Swing foot basic motion during single support: timing law $p(t)$, foot z-coordinate $z_m(t)$.

Moreover, due to the particular choice of the swing foot trajectory (17), the ZMP swing foot contribution remains linear in the decision variables x^j_f and x^{j-2}_f

$$x_{\mathrm{z},m} = x^j_\mathrm{f} \left(1 - p + \frac{z_m}{g + \ddot{z}_m} \ddot{p}\right) + x^{j-2}_\mathrm{f} \left(p - \frac{z_m}{g + \ddot{z}_m} \ddot{p}\right) \tag{19}$$

Note that x^j_f represents a control variable only for $j \geq 1$ since x^0_f is the position of the current support foot and x^{-1}_f is the starting position of the current swinging foot. Using (19) we can finally rewrite the ZMP constraint (16) as

$$\frac{1}{1 + \sigma^{k+i}} x^{k+i}_{\mathrm{z},M} + \frac{\sigma^{k+i}}{1 + \sigma^{k+i}} x^{k+i}_{\mathrm{z},m} - x^j_\mathrm{f} + \leq \frac{1}{2} x^{\max}_\mathrm{z} \tag{20}$$

where $\sigma^{k+i} = m(\ddot{z}^{k+i}_m + g)/(Mg)$. This constraint has to be verified at each sampling instant corresponding to single support phases over T_h. Note that in order to keep the constraints linear we did not consider the double support phase; this limitation can however be removed.

The stability constraint, introduced in [19],

$$\frac{1}{\omega_M} \frac{1 - e^{\delta\omega_M}}{1 - e^{N\delta\omega_M}} \sum_{i=1}^{N} e^{i\delta\omega_M} \dot{x}^{k+i}_{\mathrm{z},M} = x^k_M + \frac{\dot{x}^k_M}{\omega_M} - x^k_{\mathrm{z},M} \tag{21}$$

guarantees that the computed x_M trajectory starting at k is bounded regardless of the choice of T_h. This constraint, computed at each iteration, is obtained by rewriting (13) in terms of the control variables samples $\dot{x}^{k+i}_{\mathrm{z},M}$. The exact computation requires knowledge of all the future evolution of the ZMP, which we can predict only within the horizon T_h, i.e. $i \leq N$. For future instants $i > N$, it is possible to assume an hypothetical periodic pattern for the ZMP which leads to the closed form geometric series used in (21). A similar expression holds for $\dot{y}^k_{\mathrm{z},M}$.

Finally we have to ensure that the proposed footsteps are admissible for the humanoid. To do this we add a feasibility constraint which defines where each footstep x^j_f can be placed with respect to the previous one x^{j-1}_f. We choose a rectangular region, although it could be represented as any convex polytope

$$\begin{pmatrix} x^j_\mathrm{f} - x^{j-1}_\mathrm{f} \\ y^j_\mathrm{f} - y^{j-1}_\mathrm{f} \end{pmatrix} \leq \pm \begin{pmatrix} 0 \\ L \end{pmatrix} + \frac{1}{2} \begin{pmatrix} x^{\max}_\mathrm{f} \\ y^{\max}_\mathrm{f} \end{pmatrix} \tag{22}$$

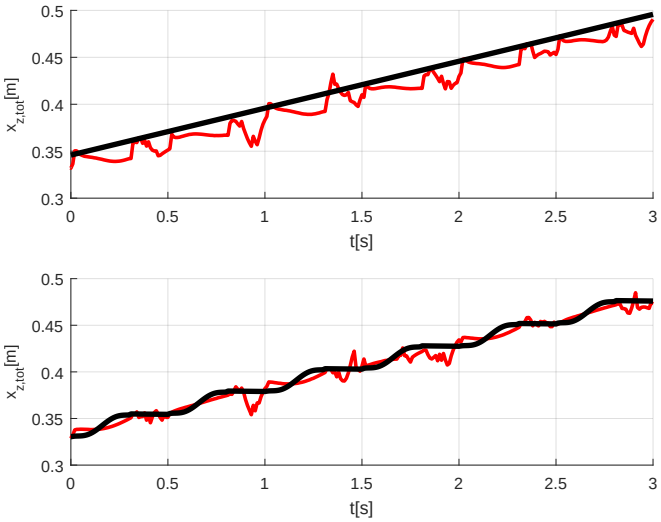

Fig. 4. LIP-based MPC with no modeling of the swinging leg (top) vs MPC for the 2-mass system (bottom): sagittal motion.

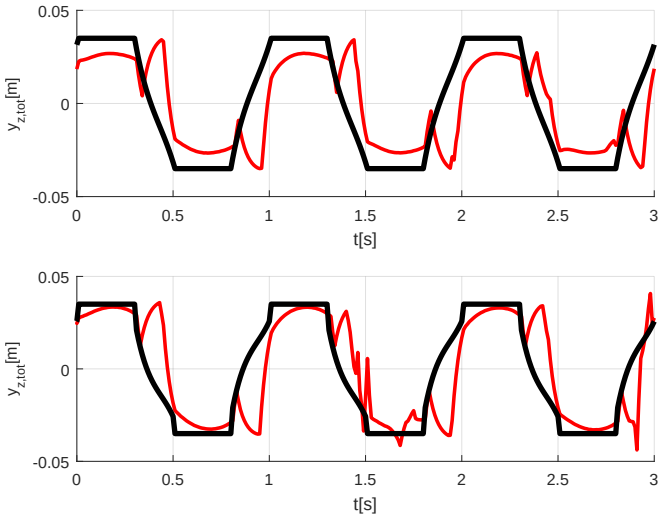

Fig. 5. LIP-based MPC with no modeling of the swinging leg (top) vs MPC for the 2-mass system (bottom): coronal motion.

Here the $\pm$ sign takes care of the difference between left and right foot, $x_{\mathrm{f}}^{\max}$ and $y_{\mathrm{f}}^{\max}$ represent the size of the admissible region while L is a reference distance between two consecutive footsteps

To simplify the exposition we did not consider any rotation of the footsteps, although these can be included by adding the proper rotation matrices in the constraints expressions.

C. Optimization problem

We look for the solution that minimizes the cost function

$$\sum_{i=1}^{N}\left(\left(\dot{x}_{\mathrm{z},M}^{k+i}\right)^2+k_{\mathrm{v}}^{x}\left(\dot{x}_{M}^{k+i}-v_x\right)^2+\left(\dot{y}_{\mathrm{z},M}^{k+i}\right)^2+k_{\mathrm{v}}^{y}\left(\dot{y}_{M}^{k+i}-v_y\right)^2\right) \tag{23}$$

subject to the ZMP constraint (20) on $x_{\mathrm{z,tot}}$, the boundedness constraint (21) and the balance constraint (22). Note that we have also included a term in the cost function that penalizes deviations from a reference velocity (v_x, v_y).

The motion of the mass m is completely defined in the single support phase because it is determined by the motion of the swinging foot. Since one mass accounts for the contribution of both legs, during the double support phase it has to go from one foot to the other to ensure the continuity of $x_{\mathrm{z},m}$. We do this by letting $x_{\mathrm{z},m}$ change linearly in the double support phase. Future implementations will consider other possibilities.

IV. Simulations and Discussion

We tested the control scheme on a NAO robot model, using the DART[2] dynamic simulator. All simulations are performed with a given sagittal reference velocity $v_x = 0.05$ m/s. We evaluated the performance of the scheme by comparing the predicted ZMP w.r.t. the actual one measured in the simulator.

In all simulations every step lasts 0.5 s with single and double support phases respectively of 0.3 s and 0.2 s. The balance constraints are squares with $x_{\mathrm{z}}^{\max} = y_{\mathrm{z}}^{\max} = 0.03$ m, while the size of the feasibility constraints is $x_{\mathrm{f}}^{\max} = 0.05$ m, $y_{\mathrm{z}}^{\max} = 0.025$ m, $L = 0.125$ m. The prediction horizon is $T_{\mathrm{h}} = 1$ s (i.e. 2 steps), and the sampling time δ is 0.01 s. The gains for the cost function are $k_{\mathrm{v}}^{x} = k_{\mathrm{v}}^{y} = 10$.

In the first set of simulations we compare a LIP-based MPC with the proposed MPC based on a 2-mass model in which the mass m accounts for 30% of the total mass. Figures 4 and 5 show that in the first case the measured ZMP is visibly different from the predicted one. The 2-mass MPC provides a better result, as the measured ZMP is closer to the predicted one during the single support phase, and the error is reduced by 35%. We don't see a significant improvement in the double support phase, which is also due to the fact that the dynamic simulator is less reliable for measuring the ZMP in a situation with multiple contact surfaces, as it produces several false values.

Figure 6 shows a comparison between four different values of the mass m, from 0% to 45% with an increase of 15% at each plot. The best fitting during the single support occurs with a value of 30% which has also been using for the previous results. Moreover it is also evident that as we continue to increase the mass m, the performance get worse as clearly shown in the 45% plot.

It is important to notice that the 0% case considers the humanoid CoM coinciding with the mass M which roughly represents the torso while the first plots in Fig. 4 and 5 represent the LIP-based MPC case where the reference is generated for the true humanoid CoM, not the torso. Moreover, by controlling M and requiring that its height remains constant, it is also evident that the true humanoid CoM will have a variable height. Indirectly, a variable height problem has been addressed by solving a constant height one.

V. Conclusions and Future Work

In this paper we have primarily shown that it is possible to use the intrinsically stable MPC framework also in the case

[2]https://dartsim.github.io/

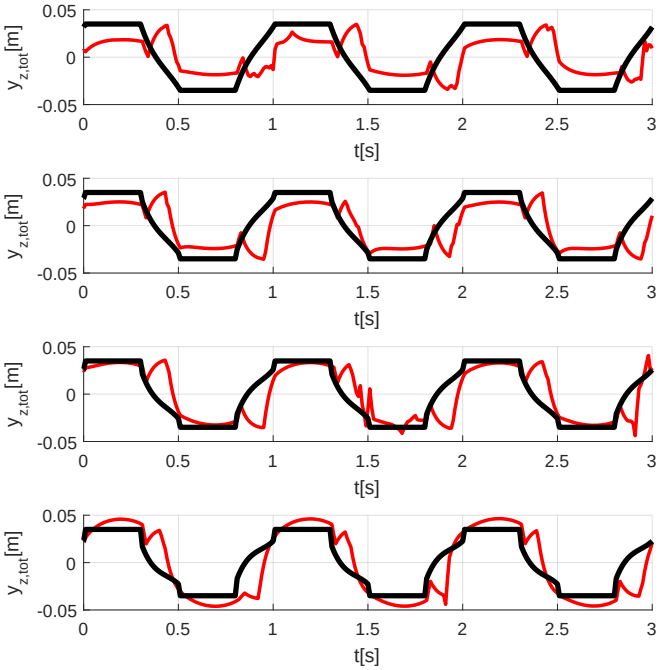

Fig. 6. 2-mass model, from the top: different values of the mass m in percentage, 0%, 15%, 30% and 45% of the total humanoid mass.

of a multi-mass humanoid model with a single primary mass and secondary masses with known motion (e.g., the swing leg). In particular a major extension has been considering the automatic footstep case where the footsteps, and therefore the swinging leg motion, are not fixed but are the outcome of the MPC solution. The experimental validation is currently scheduled together with a deeper analysis of the swinging foot trajectories and the double support phase.

REFERENCES

[1] M. Vukobratovic and D. Juricic, "Contribution to the synthesis of biped gait," *IEEE Transactions on Biomedical Engineering*, vol. BME-16, no. 1, pp. 1–6, 1969.

[2] K. Nishiwaki and S. Kagami, "Simultaneous planning of com and zmp based on the preview control method for online walking control," in *11th IEEE-RAS International Conference on Humanoid Robots*, 2011, pp. 745–751.

[3] A. Herdt, H. Diedam, P.-B. Wieber, D. Dimitrov, K. Mombaur, and M. Diehl, "Online walking motion generation with automatic footstep placement," *Advanced Robotics*, vol. 24, no. 5-6, pp. 719–737, 2010.

[4] S. Kajita, H. Hirukawa, K. Harada, and K. Yokoi, *Introduction to Humanoid Robotics*. Springer Publishing Company Inc., 2014.

[5] A. Takanishi, M. Tochizawa, T. Takeya, H. Karaki, and I. Kato, "Realization of dynamic biped walking stabilized with trunk motion under known external force," in *Proceedings of the 4th International Conference on Advanced Robotics*, K. J. Waldron, Ed. Springer Berlin Heidelberg, 1989, pp. 299–310.

[6] A. Takanishi, M. Tochizawa, H. Karaki, and I. Kato, "Dynamic biped walking stabilized with optimal trunk and waist motion," in *IEEE/RSJ International Workshop on Intelligent Robots and Systems*, 1989, pp. 187–192.

[7] J. Park and K. Kim, "Biped robot walking using gravity-compensated inverted pendulum mode and computed torque control," in *IEEE International Conference on Robotics and Automation*, vol. 4, May 1998, pp. 3528–3533.

[8] A. Albert and W. Gerth, "Analytic path planning algorithms for bipedal robots without a trunk," *Journal of Intelligent and Robotic Systems*, vol. 36, no. 2, pp. 109–127, Feb 2003.

[9] K. Erbatur and U. Seven, "An inverted pendulum based approach to biped trajectory generation with swing leg dynamics," in *7th IEEE-RAS International Conference on Humanoid Robots*, 2007, pp. 216–221.

[10] T. Buschmann, S. Lohmeier, M. Bachmayer, H. Ulbrich, and F. Pfeiffer, "A collocation method for real-time walking pattern generation," in *7th IEEE-RAS International Conference on Humanoid Robots*, 2007, pp. 1–6.

[11] T. Takenaka, T. Matsumoto, and T. Yoshiike, "Real time motion generation and control for biped robot -1st report: Walking gait pattern generation-," in *IEEE/RSJ International Conference on Intelligent Robots and Systems*, 2009, pp. 1084–1091.

[12] T. Ha and C.-H. Choi, "An effective trajectory generation method for bipedal walking," *Robotics and Autonomous Systems*, vol. 55, no. 10, pp. 795–810, 2007.

[13] S. Shimmyo, T. Sato, and K. Ohnishi, "Biped walking pattern generation by using preview control based on three-mass model," *IEEE Transactions on Industrial Electronics*, vol. 60, no. 11, pp. 5137–5147, Nov 2013.

[14] L. Lanari and S. Hutchinson, "Inversion-based gait generation for humanoid robots," in *IEEE/RSJ International Conference on Intelligent Robots and Systems*, 2015, pp. 1592–1598.

[15] ——, "Planning desired center of mass and zero moment point trajectories for bipedal locomotion," in *15th IEEE-RAS International Conference on Humanoid Robots*, 2015, pp. 637–642.

[16] L. Lanari, S. Hutchinson, and L. Marchionni, "Boundedness issues in planning of locomotion trajectories for biped robots," in *14th IEEE-RAS International Conference on Humanoid Robots*, 2014, pp. 951–958.

[17] A. Herdt, "Model predictive control of a humanoid robot," Ph.D. dissertation, Ecole nationale superieure des mines de Paris, 2010.

[18] R. C. Luo and C. C. Chen, "Biped walking trajectory generator based on three-mass with angular momentum model using model predictive control," *IEEE Transactions on Industrial Electronics*, vol. 63, no. 1, pp. 268–276, Jan 2016.

[19] N. Scianca, M. Cognetti, D. De Simone, L. Lanari, and G. Oriolo, "Intrinsically stable MPC for humanoid gait generation," in *16th IEEE-RAS International Conference on Humanoid Robots*, 2016, pp. 101–108.

[20] D. D. Simone, N. Scianca, P. Ferrari, L. Lanari, and G. Oriolo, "MPC-based humanoid pursuit-evasion in the presence of obstacles," in *IEEE/RSJ International Conference on Intelligent Robots and Systems*, 2017, pp. 5245–5250.

[21] K. Harada, S. Kajita, H. Saito, M. Morisawa, F. Kanehiro, K. Fujiwara, K. Kaneko, and H. Hirukawa, "A humanoid robot carrying a heavy object," in *2005 IEEE International Conference on Robotics and Automation*, April 2005, pp. 1712–1717.

[22] K. Hashimoto, Y. Sugahara, C. Tanaka, A. Ohta, K. Hattori, T. Sawato, A. Hayashi, H. o. Lim, and A. Takanishi, "Unknown disturbance compensation control for a biped walking vehicle," in *IEEE/RSJ International Conference on Intelligent Robots and Systems*, Oct 2007, pp. 2204–2209.

[23] D. J. Agravante, A. Sherikov, P. B. Wieber, A. Cherubini, and A. Kheddar, "Walking pattern generators designed for physical collaboration," in *IEEE International Conference on Robotics and Automation*, May 2016, pp. 1573–1578.

[24] Q. Huang, K. Yokoi, S. Kajita, K. Kaneko, H. Arai, N. Koyachi, and K. Tanie, "Planning walking patterns for a biped robot," *IEEE Transactions on Robotics and Automation*, vol. 17, no. 3, pp. 280–289, Jun 2001.

[25] H. F. Al-Shuka, B. J. Corves, B. Vanderborght, and Z. Wen-Hong, "Zero-moment point-based biped robot with different walking patterns," *International Journal of Intelligent Systems and Applications*, vol. 7, no. 1, p. 31, 2014.